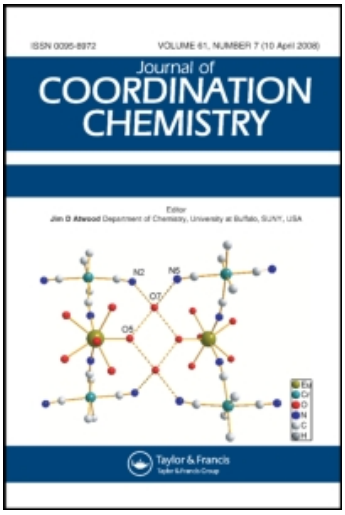

Journal of Coordination Chemistry
Publication details, including instructions for authors and subscription information:
http://www.informaworld.com/smpp/title~content=t713455674

Ligational and analytical applications of a uracil derivative toward some transition metal ions

Sahar I. Mostafa[a]; M. A. Kabil[a]; E. M. Saad[a]; A. A. El-Asmy[a]
[a] Chemistry Department, Faculty of Science, Mansoura University, Mansoura, Egypt

To cite this Article Mostafa, Sahar I. , Kabil, M. A. , Saad, E. M. and El-Asmy, A. A.(2006) 'Ligational and analytical applications of a uracil derivative toward some transition metal ions', Journal of Coordination Chemistry, 59: 3, 279 — 293
To link to this Article: DOI: 10.1080/00958970500266149
URL: http://dx.doi.org/10.1080/00958970500266149

Journal of Coordination Chemistry
Vol. 59, No. 3, 15 February 2006, 279–293

Taylor & Francis
Taylor & Francis Group

Ligational and analytical applications of a uracil derivative toward some transition metal ions

SAHAR I. MOSTAFA, M. A. KABIL,
E. M. SAAD and A. A. EL-ASMY*

Chemistry Department, Faculty of Science,
Mansoura University, Mansoura, Egypt

(*Received 29 November 2004; revised 21 February 2005; in final form 12 July 2005*)

New complexes of the uracil derivative (5,6-diamino-2,4-dihydroxypyrimidine) hemisulfate (H_2AHP) having the formulas $[Fe(HAHP)_2Cl(H_2O)]H_2O$, $[M(HAHP)_2(H_2O)_2]MeOH$ (M = Co, Ni), $[Cu(HAHP)(H_2AHP)(H_2O)Cl]H_2O$, $[Zn(HAHP)_2]H_2O$, $[MoO_2(HAHP)_2]4H_2O$, $[Ru(HAHP)_2(H_2O)_2]$, $[Rh(HAHP)_2(H_2O)Cl]$, $[Pd(AHP)_n]H_2O$, $[Ag_2(H_2AHP)(H_2O)_4](NO_3)_2$ and $[Au(H_2AHP)Cl_3]H_2O$ have been characterized by IR, electronic, ^{1}HNMR and mass spectral studies, magnetic and thermal measurements. Cyclic voltammetry was used to study the electrochemical behavior of the Ru and MoO_2 complexes. Formation of complexes in solution was studied pH metrically and their stability constants clearly indicate that the divalent metal ions have the order: Pd(II) > Cu(II) > Co(II) ~ Ni(II) > Zn(II) while Ru(III) > Rh(III) > Au(III) > Fe(III) is the order of the trivalent ions. A flotation procedure for the separation of Ag(I), Pd(II), Pt(IV) and Au(III) individually or in combination has been described. The maximum separation of each analyte is achieved using 2×10^{-4} M H_2AHP and 1×10^{-3} M oleic acid. The procedure is applied to some synthetic mixtures and the separation mechanism is proposed.

Keywords: Uracil; Complexes; Spectra; Thermal analysis; Separation flotation; Recovery

1. Introduction

The pyrimidine ring represents one constituent of nucleic acid, vitamins, coenzymes and antibiotics and provides potential binding sites for metal ions. The coordination properties of pyrimidines are important in understanding the role of metal ions in biological systems [1]. The physiological importance of pyrimidine and 2-aminopyrimidine creates great interest in complex formation [2]. 5-Bromouracil (mutagenic agent) is used in various biological systems [3]. Some gold(I,III) complexes with uracil derivatives have been used as antitumor agents vivo [4]. Numerous metal complexes containing 6-amino-5-nitroso- derivative have been isolated and characterized by spectroscopic and thermal techniques [5]. The mixed-ligand complexes of

*Corresponding author. Tel.: +2/0101645966. Email: aelasmy@yahoo.com

Journal of Coordination Chemistry
ISSN 0095-8972 print: ISSN 1029-0389 online © 2006 Taylor & Francis
DOI: 10.1080/00958970500266149

6-amino-1,3-dimethyl-5-nitrosouracil and 6-amino-1,3-dimethyl-5(2-carboxyphenyl) azouracil with Cu(II) have been reported and their X-ray crystal structures have been discussed [6–10]. Also, complexes of 5-nitrosouracil derivatives with Ag(I) have been isolated and characterized [11]. The uracil moiety is one of the important nucleobase residues in nucleotides and nucleic acids [12]. It is reported that tetrakis(1-methyl-uracilato) palladium complexes have the ability to capture alkali metal ions [13]. Schiff-base complexes derived from 2,6-diformyl-4-methylphenol and 5-aminouracil have been prepared and their biological activities determined [14].

The flotation separation process shows promise for removing toxic metal ions from dilute aqueous solutions [15–18]. Several flotation procedures for separation and recovery of Cu(II) [15, 19, 20], Co(II) [18, 20], Ni(II) [15, 18–20], Zn(II) [17], Cd(II) [17–19], Pb(II) [16, 19] and Au(III) [21] have been reported. Recently, the separation of ultra fine particles of whey protein by aphron has been reported [22].

Here, the synthesis, spectroscopy, electrochemical and thermal behavior of metal complexes with H_2AHP were reported. The stability constants have been identified and metal ions with high stability [Ag(I), Pd(II), Pt(IV) and Au(III)] were found more suitable for separation by flotation.

2. Experimental

All chemicals used in this work were analytical reagent grade. The ligand was used as supplied.

2.1. *Preparation of complexes*

2.1.1. $[Fe(HAHP)_2(H_2O)Cl]H_2O$. A 25 mL ethanol solution of $FeCl_3 \cdot 6H_2O$ (0.135 g, 0.5 mmol) was added to a 25 mL aqueous solution of H_2AHP (0.3 g, 1.5 mmol) sodium hydroxide (0.06 g, 1.5 mmol) with continuous stirring. A blue green precipitate was produced followed by a brown precipitate.

2.1.2. $[M(HAHP)_2(H_2O)_2]MeOH$ (M = Co, Ni). The acetate salt of Co(II) or Ni(II) (0.5 mmol) in 30 mL water was added to 30 mL methanol–water (1 : 2) of H_2AHP (0.2 g, 1 mmol). The solution mixture was heated under reflux for 4 h and the solution was evaporated until formation of orange precipitate.

2.1.3. $[Cu(H_2AHP)(HAHP)Cl(H_2O)] \cdot H_2O$. To a 25 mL suspension of H_2AHP (0.1 g, 0.5 mmol), $CuCl_2 \cdot 2H_2O$ (0.1 g, 0.5 mmol) in 25 mL ethanol–water (1 : 1) was added. The reaction mixture was boiled under reflux for 3 h until the formation of a greenish brown precipitate.

2.1.4. $[Zn(HAHP)_2] \cdot H_2O$. $Zn(NO_3)_2 \cdot 6H_2O$ (0.1 g, 0.5 mmol) in 25 mL water was added to H_2AHP (0.1 g, 0.5 mmol) in 25 mL ethanol–water (1 : 1 ratio). The reaction mixture was refluxed for 3 h and evaporated until a yellow precipitate formed.

2.1.5. $[MoO_2(HAHP)_2] \cdot 4H_2O$. Twenty millilitres of an aqueous solution of $(NH_4)_2MoO_4$ (0.098 g, 0.5 mmol) was added to 30 mL aqueous ethanol solution (1 : 1)

of H_2AHP (0.1 g, 0.5 mmol) and refluxed for 3 h, upon evaporation, a yellow precipitate is obtained.

2.1.6. $[Ru(HAHP)_2(H_2O)_2]$ and $[Rh(HAHP)_2Cl(H_2O)]$. $RuCl_3 \cdot 3H_2O$ (0.104 g, 0.5 mmol) or $RhCl_3 \cdot 3H_2O$ (0.16 g, 0.5 mmol) was added to a 30 mL aqueous solution of sodium acetate (0.164 g, 2 mmol) and 20 mL of H_2AHP (0.383 g, 4 mmol) with heating and stirring. The mixture was refluxed for about 4 h and a dark violet precipitate (Ru) or yellow precipitate (Rh) was isolated.

2.1.7. $[Pd(AHP)]_n \cdot H_2O$. A 10 mL aqueous solution of $K_2[PdCl_4]$ (0.16 g, 0.5 mmol) was stirred overnight with a 30 mL suspension of H_2AHP (0.2 g, 1 mmol) in water. A yellow precipitate formed.

2.1.8. $[Ag_2(H_2AHP)(H_2O)_4](NO_3)_2$. A 10 mL aqueous solution of $AgNO_3$ (0.1 g, 0.5 mmol) was added to H_2AHP (0.1 g, 0.5 mmol). The mixture was kept in the dark overnight with stirring and a pale-blue precipitate is obtained.

2.1.9. $[Au(H_2AHP)Cl_3] \cdot H_2O$. Auric acid (0.17 g, 0.5 mmol) in 20 mL water was added to a mixture of H_2AHP (0.2 g, 1 mmol) and sodium acetate (0.082 g, 1 mmol) in 20 mL water–ethanol (1 : 1) ratio. The reaction mixture was stirred with gentle heating until a beige precipitate formed.

In all the aforementioned methods, the formed precipitates were filtered off, washed several times with hot bidistilled water, ethanol, diethylether and finally dried *in vacuo*.

2.2. *pH-metric titration*

The protonation constants of H_2AHP and the formation constants of its complexes at 298.05 K were determined pH-metrically [23]. The following solution mixtures (25 mL) are titrated pH-metrically with standardized sodium hydroxide solution (0.017 M) at constant ionic strength (0.05 M KCl or KNO_3): (A) 5 mL H_2AHP (2.5×10^{-3} M) + 1.2 mL KCl (B) Mixture (A) + 0.5 or 1 mL of (1×10^{-3} M) metal ion.

2.3. *Separation and flotation*

Into a flotation cell [24], 1 mL each of Ag(I), Pd(II), Pt(IV) or Au(III) (5×10^{-5} M) is mixed with 2 mL of H_2AHP (1×10^{-4} M) and 5 mL bidistilled water. The pH was adjusted to the optimum value for each analyte by adding drops of dilute solution of either HNO_3 or NaOH and the solution was adjusted to 10 mL with bidistilled water. The cell was shaken for a few seconds to ensure complete complexation. HOL (3 mL, 1×10^{-3} M) was added and the cell was inverted by hand to ensure complete flotation. After 5 min, the scum was filtered off and the concentration of the analyte in both the mother liquor and scum was determined by flame atomic absorption or spectrophotometrically [20].

2.3.1. Simultaneous separation and microdetermination of Ag(I), Pd(II), Pt(IV) and Au(III). The same procedure for separation and flotation was applied using 0.5 mL each of Ag(I), Pd(II), Pt(IV) and Au(III) (5×10^{-5} M) and 3 mL of H_2AHP (2.5×10^{-3} M). The scum was filtered off and the filtrate was introduced to the

spectrophotometer at 330 nm [Pd(II) determination]. The precipitate containing Ag(I), Pt(IV) and Au(III) was washed three times with 10 mL of diethylether, dissolved in concentrated HNO_3 (3 mL) and heated gently to near dryness. The solution was transferred to a 10 mL volumetric flask and completed with bidistilled water. Ag(I), Au(III) and Pt(IV) were measured in the presence of 0.01 M *n*-butylamine as a flame chemical modifier by atomic absorption at 323, 237 and 260 nm, respectively.

2.3.2. Recovery of precious elements. 0.5 M of Ag(I), Pd(II), Au(III) and Pt(IV) was added to different water samples in the presence of 0.001 M H_2AHP and 0.001 M HOL at pH 4. The above procedure of separation and determination was carried out. In the recovery of pure elements, different concentrations of Ag(I), Pd(II), Au(III) and Pt(IV) (10, 20, 30 mg) in the presence of 0.5 M H_2AHP and 0.005 M HOL at pH 4 were applied.

2.4. *Instrumentation*

The IR (KBr discs), electronic (DMSO), ^{1}H NMR (d_6-DMSO) and mass spectra were measured using Matson 5000 FTIR, Unicam UV_2, Varian Gemini (200 MHz) and Varian MAT 311 Spectrometers, respectively. The TG analysis (20–1000°C) was carried out with heating rate of 10°C min^{-1} using α-Al_2O_3 as a reference on a Shimadzu Thermogravimetric Analyzer (TGA-50). The molar conductivity was measured on a YSI Model 32 conductivity bridge. Cyclic voltammetry was performed on a Potentiostat wave generator (Oxford) equipped with a 7000 AM X-Y recorder. The electrochemical cell consists of a spiral Pt wire (0.5 mm diam) as auxiliary electrode, with glassy carbon and Ag/AgCl as working and reference electrodes, respectively. The magnetic moments were evaluated at room temperature using a Johnson Matthey magnetic susceptibility balance, UK. Microanalyses were carried out at the Microanalytical Unit, Cairo University, Egypt. The pH readings were performed using a Metrohm E536 potentiograph equipped with a Dosimat (Metrohm, Herisau, Switzerland). The concentration of metal ions was determined using a Perkin-Elmer 2380 atomic absorption spectrometer with air-acetylene flame.

3. Results and discussion

Elemental analyses and some physical properties of the isolated complexes are listed in table 1. The data obtained are in agreement with the suggested formulas. The molar conductivity values for the complexes in DMSO showed them to be non-electrolytes [25].

The IR spectrum of H_2AHP exhibited absorption bands at 3414, 3392, 3294, 3157, 1711 and 1647 cm^{-1} attributed to $\nu_s(NH_2)$, $\nu_{as}(NH_2)$, ν[N(1)H], ν[N(3)H], ν[C(2)=O] and ν[C(4)=O], respectively, revealing the existence of the ligand in the keto form (figure 1a). The absorption bands appearing at 1102 and 1054 cm^{-1} are mainly due to the sulfate group which disappear in the spectra of all complexes.

Table 1. Analytical, magnetic moments and molar conductances of H_2AHP complexes.

Complex	Color	Found % (Calcd) C	H	N	M	μ_{eff} (B.M.)	Λ^a
$[Fe(HAHP)Cl(H_2O)]\cdot H_2O$	Brown	23.0 (23.4)	4.2 (3.5)	27.0 (27.3)	13.1 (13.7)	3.70	–
$[Co(HAHP)_2(H_2O)_2]\cdot MeOH$	Orange	26.9 (26.4)	3.6 (4.4)	27.0 (27.3)	14.8 (14.4)	4.97	–
$[Ni(HAHP)_2(H_2O)_2]\cdot MeOH$	Orange	26.7 (26.4)	4.0 (4.4)	27.5 (27.4)	14.8 (14.4)	2.86	–
$[Cu(HAHP)(H_2AHP)Cl(H_2O)]$	Greenish-Brown	23.5 (23.0)	3.2 (3.6)	26.3 (26.8)	15.0 (15.2)	1.50	–
$[Zn(HAHP)_2]\cdot H_2O$	Yellow	27.0 (26.3)	3.5 (3.3)	31.0 (30.7)	18.1 (17.9)	0.00	–
$[MoO_2(HAHP)_2]\cdot 4H_2O$	Yellow	19.5 (19.9)	3.1 (3.8)	23.5 (23.2)		0.00	–
$[Ru(HAHP)_2(H_2O)_2]$	Violet	23.2 (22.9)	2.9 (3.3)	26.1 (26.7)		0.00	15.0
$[Rh(HAHP)_2(C1)(H_2O)]$	Yellow	22.4 (21.9)	3.2 (3.4)	25.9 (25.0)		0.00	12.1
$[Pd(AHP)]_n\cdot H_2O$	Brown	20.0 (19.5)	2.3 (1.6)	23.4 (22.7)		0.00	8.0
$[Ag_2(H_2AHP)_2(H_2O)_4](NO_3)_2$	Blue	8.0 (8.6)	3.0 (2.6)	13.9 (14.3)		0.00	–
$[Au(H_2AHP)Cl_3]\cdot H_2O$	Paige	10.5 (10.3)	2.0 (1.9)	12.8 (12.1)		0.0	–

[a]$Ohm^{-1}\,cm^2\,mol^{-1}$.

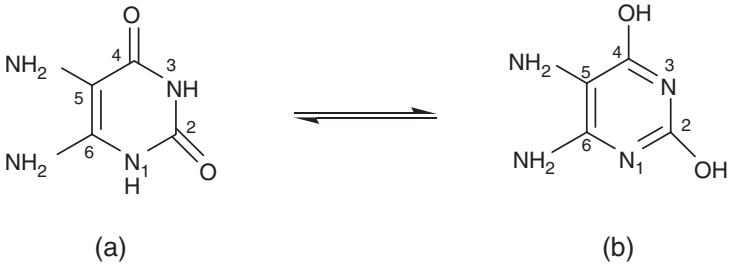

Figure 1. Structure of H_2AHP.

3.1. *Characterization of $[M(HAHP)_2(H_2O)_2]MeOH$, $[Ru(HAHP)_2(H_2O)_2]$ and $[Rh(HAHP)_2(H_2O)Cl]$*

H_2AHP acts as a mononegative bidentate ligand, coordinating to the metal ions through the deprotonated enolic carbonyl oxygen [C(4)–O] and the amino nitrogen [N(5)H_2] [26, 27]. This mode of chelation (figure 2) is based on the shift of $\nu_{as}(NH_2)$ to lower wavenumber (3188 cm^{-1}) which overlapped with ν[N(1)H] appearing together as broad band at 3157 cm^{-1}. The weak bands, observed at their initial positions, for $\nu_s(NH_2)$ and $\nu_{as}(NH_2)$ suggest the participation of only one NH_2 group in complexation. The disappearance of the bands due to ν[N(3)H] and ν[C(4)–O] indicates enolization while the other carbonyl band remains unchanged.

The ^1H NMR spectra of Ru(II) and Rh(III) complexes are similar and showed good resolution indicating that the two complexes are diamagnetic indicating Ru(III) is

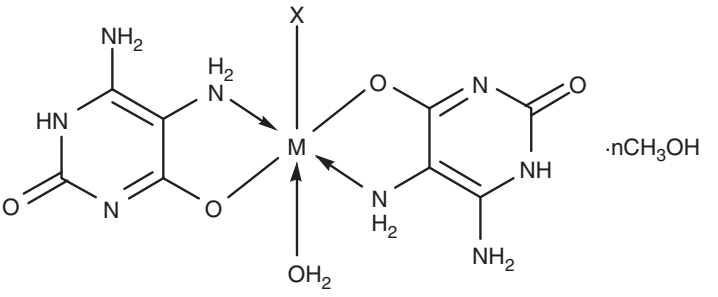

where M = Ru(II); $[Ru(HAHP)_2(H_2O)_2]$
Co(II); $[Co(HAHP)_2(H_2O)_2]MeOH$
Ni(II); $[Ni(HAHP)_2(H_2O)_2]MeOH$
Rh(III); $[Rh(HAHP)_2(H_2O)Cl]$

Figure 2. Structure of Co(II), Ni(II), Ru(II) and Rh(III) complexes.

reduced to Ru(II) upon complexation [28]. The spectra showed downfield shift of the signals of one NH_2 group at δ 6.4 and 7.3 ppm (at δ 6.10 and 6.15 ppm in H_2AHP spectrum). Also, the spectra showed a downfield shift of the NH proton at δ 11.5 ppm (at 10.5 ppm in H_2AHP) indicating its chelation with Ru(II) and Rh(III). The signal observed at δ 5.4 ppm is attributed to the protons of the coordinated water.

$[Co(HAHP)_2(H_2O)_2]CH_3OH$ starts its thermal decomposition at 50°C and includes four stages ending with cobalt. The thermogram of the Ni(II) complex showed three endothermic peaks ending with NiO, 19.1% in agreement with the calculated value (18.3%). The Rh(III) complex gives Rh_2O_3 as end product. The T.G. thermogram of $[Ru(HAHP)_2(H_2O)_2]$ showed peaks with weight loss of 9.45% (Calcd 8.6%), 14.0% (Calcd 13.6%), 30.6% (Calcd 29.8%) and 22.7% (Calcd 22%) corresponding to the release of the two coordinated water molecules, CHN_2O, $C_4H_5N_4O$ and $C_2H_4N_2O_2$ moieties, respectively. The final decomposition stage leaves Ru metal at temperature above 800°C, 22.4% (Calcd 24.0%).

The electronic spectrum of the Ru(II) complex in DMSO shows three bands at 17 545 ($^1A_{1g} \rightarrow {}^1T_{1g}$), 25 215 ($^1A_{1g} \rightarrow {}^1T_{2g}$) and 27 855 cm^{-1} (π–d_π) [29] suggesting a low-spin octahedral arrangement around the diamagnetic Ru(II) ion [30]. The electronic spectrum of the Rh(III) complex exhibited 16 670, 19 050 and 22 820 cm^{-1} bands, assigned to $^1A_{1g} \rightarrow {}^3T_{1g}$, $^1A_{1g} \rightarrow {}^1T_{1g}$ and $^1A_{1g} \rightarrow {}^3T_{2g}$ transitions, respectively, in agreement with Rh(III) in a low-spin, octahedral geometry [31]. The magnetic moments of the Co(II) and Ni(II) complexes are 4.97 and 2.86 B.M., respectively, typical values for three and two unpaired electrons, respectively. The electronic spectrum of the Co(II) complex showed two bands at 17 545 and 20 445 cm^{-1} attributed to the $^4T_{1g} \rightarrow {}^4A_{2g}$ (ν_2) and $^4T_{1g} \rightarrow {}^4T_{2g}$ (ν_3) transitions, respectively. The ligand field parameters, B (787 cm^{-1}), β (0.81) and Dq (964 cm^{-1}) are similar to those reported for octahedral geometry [31]. The electronic spectrum of the Ni(II) complex exhibited two bands at 16 670 and 23 585 cm^{-1} due to the $^3A_{2g} \rightarrow {}^3T_{1g}(F)$ and $^3A_{2g} \rightarrow {}^3T_{2g}$ transitions, respectively. The B (711 cm^{-1}), β (0.68) and Dq (953 cm^{-1}) are typical for octahedral Ni(II) [32].

The electrochemical behavior of the Ru(II) complex in $(CH_3)_4N^+Cl^-$–DMSO is investigated by cyclic voltammetry *versus* Ag/AgCl. The voltammogram showed

a cathodic wave at −0.50 V coupled with an anodic wave at −0.35 V. Another anodic peak is observed at 0.8 V coupled with a cathodic peak at 0.2 V. The wave at 0.8 V is assigned to $Ru^{(II)}/Ru^{(III)}$ while that in the reverse scan at 0.2 V is assigned to $Ru^{(III)}/Ru^{(II)}$. The $E_{1/2}$ (0.5 V) is in good agreement with that reported for the other Ru(II) complexes [33].

3.2. *Characterization of Mo, Fe and Zn complexes*

In these complexes, the ligand behaves as mononegative bidentate coordinating through the deprotonated carbonyl oxygen [C(2)–O] and the pyrimidine nitrogen [N(3)H]. These features were supported by the existence of the ν_{as} and $\nu_s(NH_2)$ bands more or less at the same position, the disappearance of ν[N(3)H] and ν[C(2)=O] with the appearance of ν[N(1)H] at 3190 cm^{-1} indicating enolization and the participation of the enolized carbonyl oxygen in bonding; the ν[C(4)=O] band exists unchanged at 1704 cm^{-1}. In $[MoO_2(HAHP)_2]4H_2O$, two extra bands at 930 and 870 cm^{-1} are assigned to ν_s and $\nu_{as}(MoO_2)$ confirming octahedral *cis*-configuration [34]. The ^1H NMR spectrum of the Zn(II) complex showed two resonances for the [N(3)H] proton at δ 11.5 and 11.9 ppm suggesting a tetrahedral *cis*-arrangement [30]. The NH_2 protons exist at the same position as in the free ligand. The anomalous magnetic moment value of the Fe(III) complex (3.7 B.M.) may be due to antiferromagnetic exchange or magnetic exchange. Its electronic spectrum exhibited one band in the visible region attributed to the $^6A_{1g} \rightarrow {}^4T_{2g}$ transition [35].

The electrochemical behavior of $[MoO_2(HAHP)_2]4H_2O$ revealed two oxidation waves at −0.26 and 0.74 V possibly assigned to $Mo^{(IV)}/Mo^{(V)}$ and $Mo^{(V)}/Mo^{(VI)}$ as irreversible electrode couples with a single electron step procedure. The reduction wave at −0.46 V *versus* Ag/AgCl is possibly assigned to the $Mo^{(VI)}/Mo^{(IV)}$ couple [36].

The thermal decomposition stages of the Fe(III) complex lead to scheme 1.

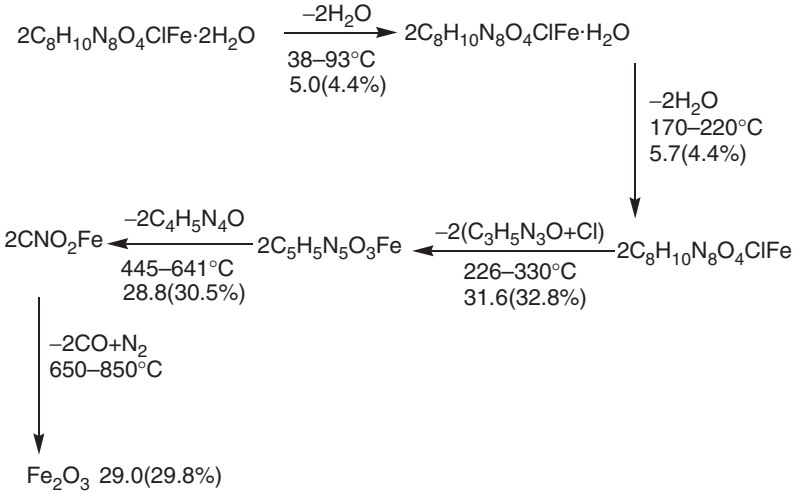

Scheme 1. Thermal decomposition of $Fe(HAHP)_2Cl(H_2O)]H_2O$.

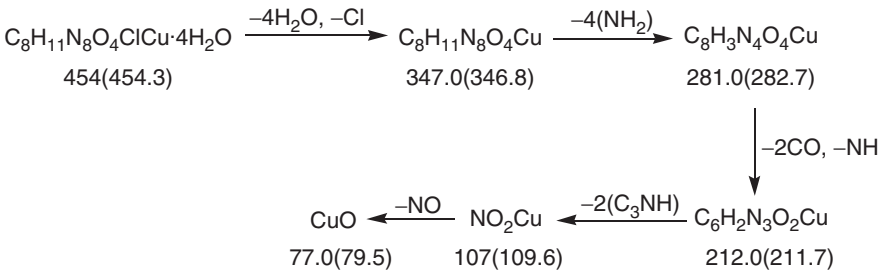

Scheme 2. Degradation of Cu(HAHP)(H_2AHP)Cl(H_2O)]H_2O using mass spectra.

3.3. *Characterization of [Cu(HAHP)(H_2AHP)Cl(H_2O)]H_2O*

This complex is a greenish brown powder with m.p. $>300^{\circ}$C, insoluble in common organic solvents but partially soluble in DMSO and DMF. Its IR spectrum showed that one ligand interacts as neutral bidentate, coordinating the Cu(II) ion through the [N(3)H] and [C(2)=O] centers; the other molecule is mononegative bidentate, coordinating the same metal ion through [N(3)H] and [C(4)=O]. This is supported by: (i) the chloride content indicates one Cl^-; (ii) the molar conductance reveals its non-electrolytic nature; (iii) the existence of the NH_2 bands more or less at the same position; (iv) the disappearance of the band at 3294 cm^{-1} with the appearance of a band at 3157 cm^{-1} strong and broad; the disappearance means deprotonation of [N(3)H] in one molecule of H_2AHP where the broadness indicates a shift of the [N(1)H] band in the other molecule to lower wavenumber overlapping with [N(3)H] and (v) the band at 278 cm^{-1} is attributed to ν(Cu–Cl) [6].

The 1.5 B.M. magnetic moment for the Cu(II) complex is lower than values reported for one unpaired electron (1.7–2.2 B.M.). The anomalous value may be due to direct metal–metal interaction [37]. The Cu(II) complex may contain two complex molecules: in the first, the two ligands are neutral while in the second they are mononegative. The mass spectrum of the Cu(II) complex showed numerous peaks representing successive degradations (scheme 2). The observed peak at $m/e = 454$ (Calcd 454.3) represents the molecular ion peak supporting the suggested formula. The base peak (100% abundance) has CuO_2N, in which the NO molecule is evolved to give CuO as a residual compound with abundance of 77%.

3.4. *Characterization of [Pd(AHP)]$_n$$H_2O$*

The reaction of K_2[$PdCl_4$] with H_2AHP yields a high intensity yellow color. The solid has 8.0 $Ohm^{-1}\,cm^2\,mol^{-1}$ molar conductance typical for non-electrolytic compounds [38]. The IR spectrum of the isolated complex showed disappearance of the bands due to ν(C=O) and ν(NH) with simultaneous appearance of new bands at 1587 and 1277 cm^{-1} attributed to ν(C=N) and ν(C–O) vibrations, respectively. This is common with the participation of two enolized carbonyl groups in bonding. The bands assigned to $\nu_s(NH_2)$, $\nu_{as}(NH_2)$ and δ (NH_2) remain more or less unaffected upon coordination. The appearance of new bands at 510 and 415 cm^{-1} due to ν(M–O) and ν(M–N) vibrations, respectively, supports oxygen and nitrogen involved in the chelation. It is suggested that H_2AHP behaves as a binegative, tetradentate ligand coordinating two

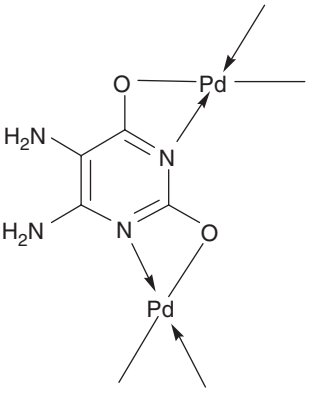

Figure 3. Structure of Pd(II) complex.

palladium ions through the pyrimidine nitrogens and the deprotonated enolic carbonyl groups from each side as shown in figure 3. The complex is square-planar configuration due to its diamagnetic behavior. Its electronic spectrum in DMF solution exhibited two bands at 20 620 and 30 300 cm^{-1} due to the $^1A_{1g} \rightarrow {}^1B_{1g}$ and $^1A_{1g} \rightarrow {}^1E_g$ transitions, respectively [39]. The T.G. thermogram of the Pd(II) complex is distinguished by three stages. The first (33–321°C) corresponds to release of water (Found 7.7%; Calcd 6.8%). The second (395–448°C) is due to elimination of $C_2N_2H_4$ moiety (Found 20.4%; Calcd 21.0) where the third stage (448–554°C) corresponds to elimination of C_2N_2 (Found 19.6%; Calcd 19.6%) leaving PdO as a final product (Found 52.8%; Calcd 52.3).

3.5. *Characterization of $[Ag_2(H_2AHP)(H_2O)_4](NO_3)_2$*

This binuclear complex is isolated from reaction of the ligand with $AgNO_3$ in the dark. The elemental analysis suggests a 2 : 1 ratio. The IR spectrum confirmed that H_2AHP coordinates through [N(1)H] and [N(6)H_2] with one metal ion and [C(4)=O] and [N(5)H_2] with the second metal ion. This suggestion is confirmed by (i) the shift of ν[N(1)H] to lower wavenumber (3100 cm^{-1}) while [N(3)H] remains unaffected indicating that [N(1)H] is a coordination site, (ii) the shift of $\nu(NH_2)$ to higher wavenumbers (3474 and 3445 cm^{-1}) and that of ν[C(4)=O] to lower wavenumber indicate the participation of both groups in chelation, (iii) the band observed at 1634 cm^{-1} is attributed to uncoordinated [C(2)=O], (iv) the new bands at 1380 and 825 cm^{-1} are due to $\nu(NO_3)$ vibrations, consistent with non-coordinated nitrate [27], (v) the appearance of bands at 3500 (sh), 870 (s) and 670(s) cm^{-1} are characteristic for coordinated water and (vi) the bands at 500, 420 and 355 cm^{-1} are due to ν(Ag–OH_2), ν(M–O) and ν(M–N) vibrations, respectively. The electronic spectrum of the Ag(I) complex showed two bands at 25 250 and 21 010 cm^{-1} attributed to the presence of Ag(I) ion in a square planar stereochemistry [39] (figure 4a).

3.6. *Characterization of $[Au(H_2AHP)Cl_3]H_2O$*

The title complex has a melting point >300°C, insoluble in common organic solvents but partially soluble in DMSO and DMF solutions. The ligand is neutral bidentate

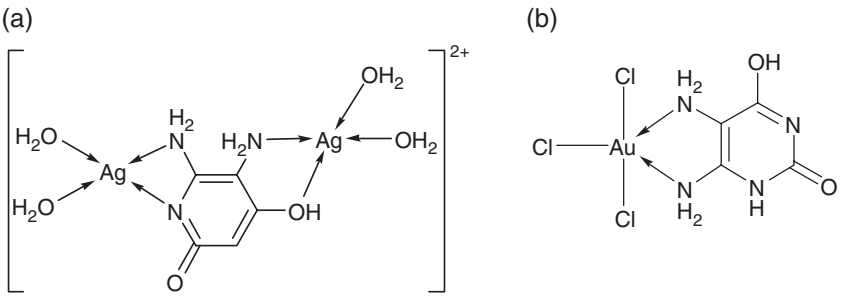

Figure 4. Structure of: (a) Ag(I) complex, (b) Au(III) complex.

coordinating via the two amino groups (figure 4b) indicated by the shift of $\nu_{as}(NH_2)$, $\nu_s(NH_2)$ and $\delta(NH_2)$ to lower wavenumbers and the disappearance of [N(1)H] with the appearance of new bands at 3536, 1582 and 1258 cm^{-1} attributed to ν(OH), ν(C=N) and ν(C–O), respectively. The appearance of ν[N(1)H] and ν[C(2)=O] at high wavenumber may be due to the formation of intramolecular hydrogen bonding and the appearance of sharp and high intensity bands at 460 and 300 cm^{-1} may be attributed to ν(M–N) and terminal ν(M–Cl) vibrations.

3.7. *pH-metric measurements*

The pH-metric titrations of 5×10^{-4} M H_2AHP with 0.017 M NaOH in absence of HCl (HCl may protonate the two amino groups in H_2AHP) and in aqueous solution at constant ionic strength ($\mu = 0.05$ M) and at room temperature ($\pm 25^{\circ}C$) were carried out using the procedure developed by Bjerrun [40]. The titrations showed that the metal–ligand curves are below that of the free ligand and well separated indicating that complexation took place with liberation of hydrogen ions. The $\overline{n}_A$, $\overline{n}$ and pL were calculated at different pH values using the Irving–Rossotti equations [24]. Plotting $\overline{n}_A$ against pH represents the protonation curve in which the values of pK calculated from the half method and the least square method are 8.95 and 6.5, respectively. The metal–ligand stability constants were evaluated from the relation between $\overline{n}$ and pL and the values are listed in table 2. The values of $\log \beta_1$ for the 1 : 1 complexes clearly indicate the following order: Pd(II) > Cu(II) > Co(II) ~ Ni(II) > Zn(II) for the divalent metal ions and Ru(III) > Rh(III) > Au(III) > Fe(III) for the trivalent metal ions.

3.8. *Separation and microdetermination of Ag, Pd, Pt and Au*

In solvent technique, oleic acid (HOL) is an excellent surfactant for selective separation of some metal ions as solids or soluble colored complexes in the scum layer [41, 42]. To float Ag(I), Pd(II), Pt(IV) and Au(III) each individually or in combination using HOL, a series of experiments were carried out. The suitable concentration of each of analyte (5×10^{-5} M) was taken in the flotation cell with sufficient quantity of HOL (1×10^{-3} M), less than the critical micelle concentration (CMC), to float the above analytes at different pH. The data prove that no more than 25, 40, 75, 80 and 80% of Pt(IV), Ag(I), Au(III), Hg(II) and Pd(II), respectively, were separated at any pH; unsatisfactory separation percentages. Accordingly, many trials were carried out to

Table 2. Deprotonation constants of H_2AHP and the formation constants of its complexes.

	Half-method			Least-square method			
Ion	pK_1	pK_2	pK_3	pK_1	pK_2	pK_3	
H^+	8.95	6.50	–	8.95	6.50	–	
M^{+n}	β_1	β_2	β_3	β_1	β_2	β_3	β^*
Fe(III)	6.40	–	–	6.30	–		6.40 (β_1)
Co(II)	4.30	–	–	4.35	–	–	4.30 (β_1)
Ni(II)	4.30	–	–	4.30	–	–	4.30 (β_1)
Cu(II)	6.20	–	–	6.20	–	–	6.20 (β_1)
Ru(III)	10.65	9.75	8.65	10.69	9.75	8.85	29.05 (β_3)
Rh(III)	10.00	9.05	6.10	10.01	9.00	6.40	26.00 (β_3)
Pd(II)	8.9	4.10	–	8.85	4.17		13.02 (β_2)
Ag(I)	4.30	–	–	4.35	–	–	4.35 (β_1)
Au(III)	7.40	4.35	–	7.25	4.40	–	11.75 (β_2)
Hg(II)	9.85	–	–	9.90	–	–	9.90 (β_1)
Zn(II)	2.55	–	–	2.50	–	–	2.55 (β_1)

β^* is the overall formation constant.

separate each analyte quantitatively and selectively; H_2DAHP was an excellent collector. The data showed that selective and complete separation (~100%) of Ag(I), Pd(II), Pt(IV) and Au(III) was obtained in the pH range 1–5.5, 1–5, 1–4, 1–7, respectively, in the presence of 1×10^{-4} M H_2AHP.

The effect of H_2AHP concentration on the flotation of the analytes was investigated (figure 5). The data showed that Ag(I), Pd(II) and Pt(IV) reach its complete separation at 1 : 1 (analyte : H_2AHP) ratio, while Au(III) reaches maximum separation at 1 : 2 ratio; excess H_2AHP has no effect. Accordingly, 2×10^{-3} M H_2AHP has been selected as suitable concentration for subsequent experiments. To confirm the data in figure 5, another series of experiments were carried out to float different solutions containing variable amounts of each analyte individually at the optimum pH to cover different ratios with H_2AHP (1×10^{-4} M) using HOL (1×10^{-3} M). The separation percentage reached 100% at both H_2AHP (0.5×10^{-4} M) and (1×10^{-4} M) concentrations for Ag(I), Pd(II), Pt(IV) and Au(III) corresponding to 1 : 2 and 1 : 1 molar ratios, respectively. Above such concentration, the separation efficiency decreased due to the presence of insufficient H_2AHP for complete complexation.

The effect of surfactant concentration on the floatability and separation of 5×10^{-5} M of Ag(I), Pd(II), Pt(IV) and Au(III) in the presence of 2×10^{-4} M H_2AHP has been studied. The flotation efficiency increases to maximum (~100%) at 1×10^{-4} M HOL and remaining constant over a wide range of HOL (5×10^{-5} M) concentration. Thus, 1×10^{-3} M was fixed throughout all measurements. Under these conditions, the flotation efficiency reached ~100% and remains constant up to 80°C for Ag(I), Pd(II), Pt(IV) and Au(III).

Table 3 summarizes the effect of ionic strength on the separation of Ag(I), Pd(II), Pt(IV) and Au(III) in the presence of H_2AHP (1×10^{-4} M) under the recommended conditions. There is no evidence of specific interaction between SO_4^{-2}, NO_3^- or Cl^- or oleate (OL^-) ions. On the other hand, Na^+, K^+, Ca^{2+} and Mg^{2+} as chloride, nitrate or sulfate salts slightly depressed the separation efficiency [20]. Also, high concentrations of $CaCl_2$ (0.5 M) significantly affect the separation, probably due to the formation of calcium oleate [20]. The analytes can be safely separated from saline water.

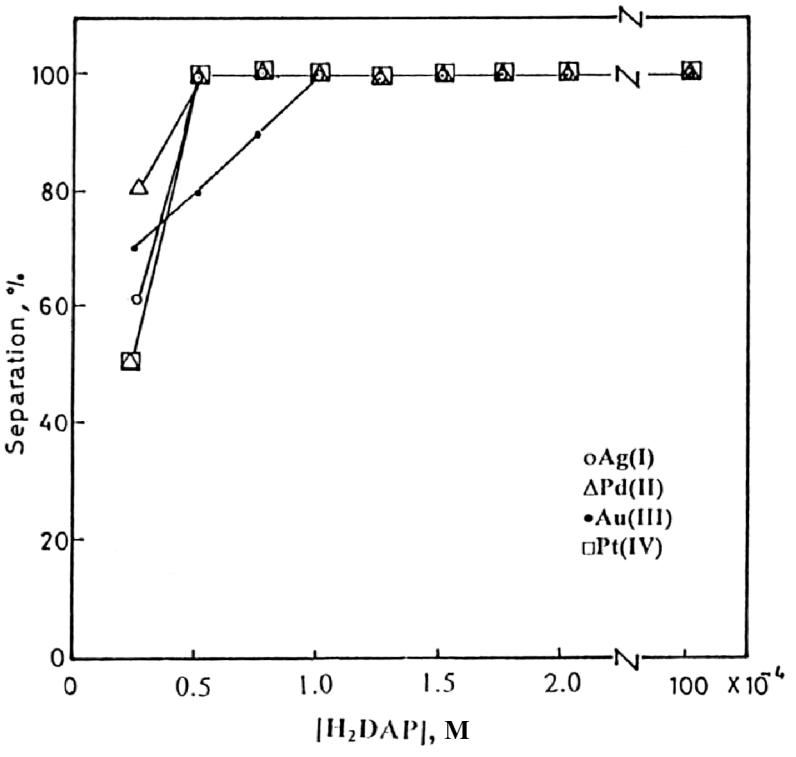

Figure 5. Effect of H_2AHP concentration on the separation of Ag(I), Pd(II), Pt(IV) and Au(III).

Table 3. Effect of ionic strength on the floatability of Ag(I), Pd(II), Pt(IV) and Au(III) using H_2AHP (2×10^{-4} M) and HOL (2×10^{-3} M) at pH 4.

		Separation (%)			
Salt	Concentration (mM)	Ag(I)	Pd(II)	Pt(IV)	Au(III)
Na	5	99	99	99	99
	100	99	99	99	99
	500	99	99	99	94
K	5	99	99	97	99
	100	99	99	99	99
	500	98	99	99	99
Mg	5	99	99	99	99
	100	99	99	99	99
	500	99	99	99	99
Ca	5	93	95	96	96
	100	90	93	94	95
	500	87	90	91	90

Possible application of this study in the selective separation of traces of Ag(I), Pd(II), Pt(IV) and Au(III), not only depends on the degree of interference from contaminants allied with the analyte but also on the control of harmful effects e.g., various ions naturally allied with the analytes individually or in combination in their samples.

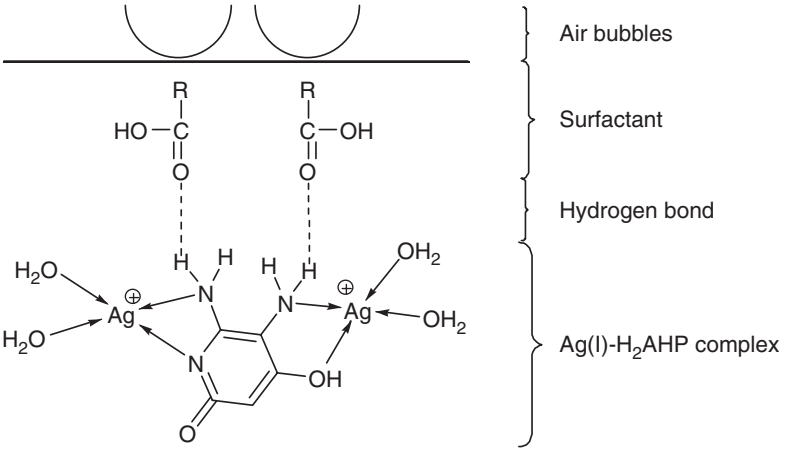

Scheme 3. The separation mechanism of Ag(I) complex.

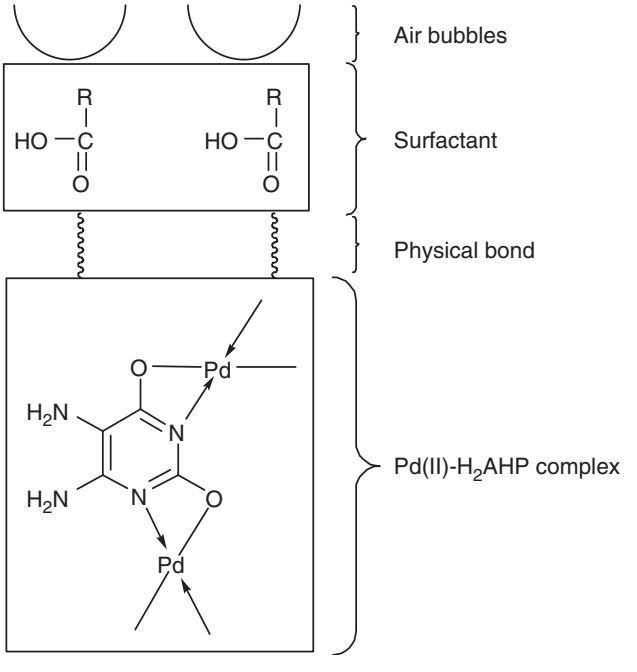

Scheme 4. The separation mechanism of Pd(II), Pt(IV) and Au(III) complexes.

It is clear that Na^{+}, K^{+}, Ba^{2+}, Ca^{2+}, Sr^{2+}, Mg^{2+}, Mn^{2+}, Pd^{2+} and Ni^{2+} individually or in combination have no pronounced effect on the separation efficiency of the analytes. For Cu^{2+}, Cr^{3+}, Fe^{3+}, Cd^{2+} and Co^{2+} interference occurs to some extent individually or in combination. These effects can be completely eliminated (except in case of Fe^{3+}) by increasing the concentration of H_2AHP to 2.5×10^{-3} mol L^{-1}. To eliminate the

Table 4. Recovery of 0.25 M of Ag(I), Pd(II), Au(III) and Pt(IV) added to different water samples in the presence of H_2AHP (1×10^{-3} M) and HOL (10^{-3} M) at pH 4.

	Mean recovery (%)			
Type of water	Ag	Pd	Au	Pt
Nile water	99.2	100	100	100
Tap water	100	100	100	100
Groud water	98.8	99.7	99.6	99.6
Mineral water	100	100	100	100

Table 5. Recovery of different concentrations of Ag, Au, Pd and Pt in the presence of H_2AHP (0.5 M) and HOL (0.005 M) at pH 4.

	Analyte recovered (mg)			
Analyte added (mg)	Ag	Au	Pd	Pt
10	9.8	9.8	2.0	2.0
20	19.7	19.9	4.0	4.0
30	29.7	29.8	6.0	6.0

interferences in case of Fe^{3+}, 0.1 M of NaF was added in the presence of 2.5×10^{-3} M H_2AHP.

The absorption spectra of Pd(II), H_2AHP, Pd–H_2AHP and Pd–H_2AHP–HOL systems have been studied. The spectrum of Pd–H_2AHP–HOL shows a band at 330 nm, which does not appear in the spectra of H_2AHP, HOL or Pd(II) species [20]. The apparent formation constants (K_f) of the soluble complexes (1 : 1 ratio) formed in the presence and absence of HOL are 9.9×10^7 and 6.2×10^6 M, respectively.

The nature of interaction between HOL and the formed complex (M–H_2AHP–HOL) has been studied to approach the actual mechanism of flotation. As the role of surfactant is very important, the elemental analyses, physical properties and spectral data of the complexes isolated in the presence and absence of oleic acid were compared. The flotation mechanism was suggested as forming a hydrogen bond between the hydrophobic part of oleic acid and the active sites in H_2AHP complex in case of Ag(I) [15, 43] and physical interaction with oleic acid [44] in Pd(II), Pt(IV) and Au(III) (schemes 3 and 4).

3.9. *Recovery of precious metals*

The data in tables 4 and 5 showed complete separation and recovery for silver and gold while palladium and platinum are partially recovered. An application for recovery of Ag from real samples (photographic emulsions) was carried out.

References

[1] D.M. Demertzi. *Bull. Chem. Soc. Jpn.*, **64**, 744 (1991).
[2] P.O. Lumme, H. Knuuttila. *Polyhedron*, **14**, 1553 (1995).
[3] U.P. Singh, R. Ghose, A.K. Ghose. *Bull. Chem. Soc. Jpn.*, **63**, 1226 (1990).
[4] R. Kivekas, E. Colacio, J. Ruiz, J.D. Lopez, P. Leon. *Inorg. Chim. Acta*, **159**, 103 (1989).

[5] J.M. Salas, M.A. Remero, M.P. Sanchez, M.N. Moreno, M. Quiros. *Polyhedron*, **11**, 2217 (1992).
[6] F. Belasnger, R. Faure, F. Hueso, M.N. Moreno, J.A. Rodriguez, J.M. Salas. *Polyhedron*, **17**, 1747 (1998).
[7] R. Kivekas, A. Pajunen, E.C. Rodriguez, J.M. Dominguez, J. Moreno, A. Romerosa. *Acta Chem. Scandinavica*, **51**, 1051 (1997).
[8] G. Ferguson, J.N. Low, M. Quiros, J.M. Salas, F. Hueso, M.N. Moreno. *Polyhedron*, **15**, 3233 (1996).
[9] J.M. Mereno, J. Ruiz, J.M. Dominguez, E. Colacio, D. Galisteo, R. Kivekas. *Polyhedon*, **13**, 203 (1994).
[10] F. Hueso, M.N. Moreno, J.M. Salas, G. Alvarez. *J. Inorg. Biochem.*, **43**, 17 (1991).
[11] J.M. Salas, M.N. Moreno, M.A. Romero, E.C. Rodriguez. *Rev. Chem. Miner.*, **21**, 233 (1984).
[12] B. Knobloch, C.P. Dacosta, W. Linert, H. Sigal. *Inorg. Chem. Comm.*, **6**, 90 (2003).
[13] M. Mizutani, S. Miwa, N. Fukushima, Y. Funahashi, T. Ozawa, K. Jitsukawa, H. Masuda. *Inorg. Chim. Acta*, **339**, 543 (2002).
[14] F.H. Uerena, N.A. Illan-Cabeza, M.N. Moreno, J.M., Martinez, M.J. Ramirez. *J. Inorg. Biochem.*, **94**, 326 (2003).
[15] F.M. Doyle, Z. Liu. *J. Colloid Interf. Sci.*, **258**, 396 (2003).
[16] K. Cundeva, T. Stafilov, G. Pavlovska. *Spect. Chim. Acta B*, **55**, 1079 (2000).
[17] C.A. Koslowski, M. Ulewicz, W. Walkowiak, T. Girek, J. Jablonska. *Min. Eng.*, **15**, 677 (2002).
[18] M. Caballero, R. Lopez, R. Cela, J.A. Perez-Bustamante. *Anal. Chim. Acta*, **196**, 287 (2000).
[19] C. Aldrich, D. Feng. *Min. Eng.*, **13**, 1129 (1987).
[20] M.A. Kabil, S.E. Ghazy, A.A. El-Asmy, Y.E. Sherif. *Fresenius J. Anal. Chem.*, **357**, 401 (1997).
[21] Z. Marczenko, K. Jankowski. *Anal. Chim. Acta*, **176**, 185 (1985).
[22] M.C. Amiri, K.T. Valsaraj. *Separat. Purif. Techn.*, **35**, 161 (2004).
[23] H.M. Irving, H.S. Rossotti. *J. Chem. Soc.*, 2904 (1954).
[24] S.E. Ghazy, M.A. Kabil. *Bull. Chem. Soc. Jpn.*, **67**, 2098 (1994).
[25] P.J. Burke, K. Henrick, D.R. McMillin. *Inorg. Chem.*, **21**, 881 (1982).
[26] M.A. Gupta, M.N. Srivastava. *Synth. React. Inorg. Met. Org. Chem.*, **26**, 305 (1996).
[27] H.E. Mabrouk, A.A. El-Asmy, M. Khalifa, M. Zedan. *Synth. React. Inorg. Met.-Org. Chem.*, **26**, 423 (1996).
[28] M.A. Romero, J.M. Salas, M. Simard, M. Quiros, A.L. Beauchamp. *Polyhedron*, **9**, 2733 (1990).
[29] J.M. Ferraro. *Low Frequency Vibrations of Inorganic and Coordination Compounds*, Plenum Press, New York (1971).
[30] Z.A. Siddiqi, S.N. Qiolawi, V.J. Mathew. *Synth. React. Inorg. Met-Org. Chem.*, **23**, 709 (1993).
[31] S.I. Mostafa. *Transition Met. Chem.*, **23**, 397 (1998).
[32] A.A. El-Asmy, M.A. Hafez, E.M. Saad, F.I. Taha. *Transition Met. Chem.*, **19**, 603 (1994).
[33] M. Armadon, R. Lena, M. Rafeal, D.R.J. Federico. *J. Coord. Chem. Rev.*, **29**, 359 (1993).
[34] S.I. Mostafa, S.A. Abd El-Maksoud. *Monats. Chem.*, **129**, 455 (1998).
[35] F. Lloret, M. Julve, J. Faus, X. Solans, Y. Journaux, I. Morgen Sterm-Badarau. *Inorg. Chem.*, **29**, 2232 (1990).
[36] T. Nyokong. *Polyhedron*, **13**, 215 (1994).
[37] S.I. Mostafa, M.M. Bekheit, M.M. El-Agez. *Synth. React. Inorg. Met. – Org. Chem.*, **30**, 2029 (2000).
[38] W.J. Geary. *Coord. Chem. Rev.*, **7**, 81 (1971).
[39] S.I. Mostafa, M.M. Bekheit. *Chem. Pharm. Bull. Jpn.*, **48**, 266 (2000).
[40] J. Bjerrum. *Metal Amine Formation Aqueous Solutions*, Hasse and Son, Copenhagen (1941).
[41] M.A. Kabil. *Fresenius J. Anal. Chem.*, **348**, 246 (1994).
[42] M.A. Kabil, S.E. Ghazy, A.M. Abeidu, N.M. El-Metwaly. *Spect. Sci. Techn.*, **30**, 3787 (1995).
[43] M.A. Kabil, M.A. Akl, A.M. Abdallah, D.S. Ismail. *Anal. Sci.*, **16**, 713 (2000).
[44] A.I. Zouboulis, K.A. Matis, N.K. Lazaridis, P.N. Golyshin. *Min. Eng.*, **16**, 1231 (2003).